

Structural, magnetic, thermodynamic, and transport properties of A-site disordered $\text{Nd}_{0.3}\text{Sm}_{0.2}\text{Sr}_{0.5}\text{MnO}_3$

N. Kumar Swamy · N. Pavan Kumar ·
Manish Gupta · S. Sanmukhrao Samatham ·
V. Ganesan · Vikas Malik · B. K. Das

Received: 27 January 2014 / Accepted: 3 June 2014 / Published online: 24 June 2014
© Akadémiai Kiadó, Budapest, Hungary 2014

Abstract The structural, magnetic, thermodynamic, and transport properties of polycrystalline sample of A-site disordered $\text{Nd}_{0.3}\text{Sm}_{0.2}\text{Sr}_{0.5}\text{MnO}_3$ were investigated in an attempt to understand the effect of substitution of Sm over well-studied parent compound $\text{Nd}_{0.5}\text{Sr}_{0.5}\text{MnO}_3$. Samples were prepared by the solid-state ceramic route method and characterized by XRD and standard iodometric titration. DC magnetization of the sample was measured by a SQUID Magnetometer. Electrical resistivity of the sample was measured by the standard four probe method. Results showed that doping with Sm allowed first-order phase transition from ferromagnetic metal to antiferromagnetic insulator state and a charge ordering at 150 K was also observed. Magnetocaloric effect studies were carried out from the specific heat data.

Keywords Manganites · First-order phase transition · Charge ordering · Magnetocaloric effect

Introduction

The manganites of the general formula $\text{Ln}_{1-x}\text{A}_x\text{MnO}_3$ (where Ln = La, Pr, Nd, Eu, Sm, Gd, Ho and A = Sr, Ca, Ba) with Ln and A occupying the rare earth A-type sites in the distorted perovskite ABO_3 structure exhibit a number of interesting phenomena like colossal magneto-resistance (CMR), insulator to metal transition, paramagnetic (PM) to ferromagnetic (FM) or antiferromagnetic (AFM) transitions, and charge-ordered (CO) states as a function of composition (x), temperature, pressure, and applied magnetic field [1, 2]. Divalent ion substitution at A-site gives rise to the ferromagnetism with metallic property followed by double exchange [3], and substitution of A-site trivalent ion with other trivalent ions leads to disorder and change in average ionic radius at A-site. If x_i , r_i and r_A are the fractional occupancies and ionic radii of A-site and the average ionic radius, the relation for variance $\langle\sigma^2\rangle$ can be written as $\langle\sigma^2\rangle = \sum x_i r_i^2 - r_A^2$ [4, 5]. Change in average ionic radius will further change the variance $\langle\sigma^2\rangle$, which plays an important role in the charge ordering and the orbital ordering state. Divalent Sr^{2+} doped $\text{Nd}_{1-x}\text{Sr}_x\text{MnO}_3$ (NSMO) has a well-known orthorhombic structure with space group—*Imma* and an average A-site cation radius $\langle r_A \rangle$ of 0.1236 nm. Interestingly, this system is metallic and ferromagnetic just below room temperature and becomes an AFM charge-ordered (CO) insulator around 150 K [1, 2]. In a large bandwidth system [3, 6], kinetic energy of the charge carriers is comparatively large and so charge order is relatively weaker (e.g., $\text{Sm}_{1-x}\text{Sr}_x\text{MnO}_3$). In a small bandwidth system, the kinetic energy of the charge carrier is comparatively smaller and charge ordering is very robust (e.g., $\text{La}_{1-x}\text{Ca}_x\text{MnO}_3$). Depending on the bandwidth, various phases are present in manganites [3]. As the tolerance factor (t) or equivalently the ionic radius of the

N. K. Swamy (✉) · M. Gupta · V. Malik · B. K. Das
Material Science Research Lab, ITM University, HUDA Sector
23A, Gurgaon 122017, Haryana, India
e-mail: nkumarswamy15@gmail.com

N. K. Swamy
School of Engineering and Research, ITM University,
New Raipur 493661, Chhattisgarh, India

N. P. Kumar
Department of Physics, Osmania University,
Hyderabad 500007, A.P., India

S. S. Samatham · V. Ganesan
Low Temperature Lab, UGC-DAE CSR, DAVV Campus,
Khandawa Road, Indore 452017, M.P., India

A-site decreases from (La/Sr) to (Pr/Ca) through (Nd/Sr), the Mn–O–Mn bond angle changes and hence bandwidth (W) of the e.g. state carrier decreases. This means that the other electronic instabilities such as the charge-ordered and orbital-ordered, and super-exchange (SE) interaction compete with the double-exchange (DE) interaction. The parent compound $\text{Nd}_{0.5}\text{Sr}_{0.5}\text{MnO}_3$ under investigation here is a lower bandwidth system [7]. Therefore, the doping with Sm having lower ionic radius ($\langle r_A \rangle$ of Sm^{3+} and Nd^{3+} are 0.109 and 0.112 nm, respectively) in this compound will decrease the average ionic radius $\langle r_A \rangle$ of the A-site. Ionic radius, related to tolerance factor t , will also decrease. Consequently, tolerance factor [8] is also related to the bandwidth of the system, i.e., on decreasing the average ionic radii, the bandwidth of the system will also decrease and the distortion will be more, and Curie temperature T_C , will also decrease with $\langle r_A \rangle$.

The CMR materials have extensively been investigated [1, 9] because of their another interesting property known as the magnetocaloric effect (MCE) [10]. MCE is defined as the thermal response of a magnetic material to an applied magnetic field and is apparent as a change in its temperature, and is quantitatively characterized either by adiabatic temperature change (ΔT) or by the isothermal magnetic entropy change (ΔS) due to a varying magnetic field. Systems showing large MCE in the low-temperature region are important for basic research as well as for specific technological applications such as space science and liquefaction of hydrogen in the fuel industry. In the view of these facts, an attempt has been made to explain the structural, magnetic, electrical, and thermodynamic properties of $\text{Nd}_{0.3}\text{Sm}_{0.2}\text{Sr}_{0.5}\text{MnO}_3$.

Experimental

The polycrystalline sample of $\text{Nd}_{0.3}\text{Sm}_{0.2}\text{Sr}_{0.5}\text{MnO}_3$ (NSSMO) was prepared by the standard solid-state reaction method. Considering the hygroscopic nature of the rare earth materials Nd_2O_3 and Sm_2O_3 , they were given a pre-heat treatment at 1,000 °C for 10 h. Stoichiometric ratios of starting chemicals Nd_2O_3 , Sm_2O_3 , SrCO_3 , and MnO_2 (all of AR grade) were taken and thoroughly mixed for 5 h using an agate mortar. The mixed powder sample was twice calcined in air at 1,200 °C for 24 h with an intermediate grinding using a ball mill and then pelletized into cylindrical shape of diameter 10 mm using a hydraulic press by applying a pressure of 1 tons cm^{-2} . The pellets were then heated at 1,300 °C for 36 h in air. Finally, these pellets were sintered at 1,450 °C for 36 h in air. The room temperature X-ray diffraction (XRD) patterns were measured by a Rigaku Dmax 300 diffractometer using the CuK_α radiation. DC magnetization measurements were

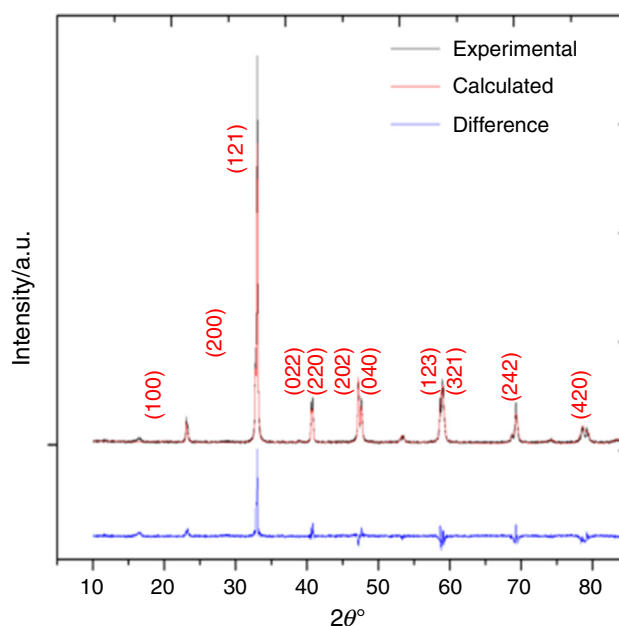


Fig. 1 X-ray diffractogram of $\text{Nd}_{0.3}\text{Sm}_{0.2}\text{Sr}_{0.5}\text{MnO}_3$ showing single phase. It also shows difference between the measured and calculated intensities

Table 1 Lattice parameters determined from Reitveld profile refinement of the powder XRD pattern of $\text{Nd}_{0.3}\text{Sm}_{0.2}\text{Sr}_{0.5}\text{MnO}_{3+\delta}$ and concentrations of Mn^{3+} and Mn^{4+} ions are given

a/nm	b/nm	c/nm	Volume/ nm^3	$\text{Mn}^{3+}/$ %	$\text{Mn}^{4+}/$ %	Mn – Valence
0.54713	0.54280	0.76318	0.22765	52.9	47.02	3.4467

The mean valence state of the Mn ion was found by Redox-iodometric titration

carried out with a Quantum Design Superconductor Quantum Interference Design (SQUID) magnetometer in the temperature range of 2–300 K. Specific heat measurements were carried out using a Physical Property Measurement System (PPMS) system at various magnetic fields in the temperature range of 2–300 K. Electrical resistivity and magnetoresistance were measured using the PPMS system in the temperature range of 2–300 K in the presence of various magnetic fields.

Results and discussion

Structural characterization

Figure 1 shows room temperature X-ray diffraction (XRD) pattern of the NSSMO sample. Diffractogram was indexed, and the sample was found to be single phase with orthorhombic pbnm symmetry. XRD pattern was analyzed by

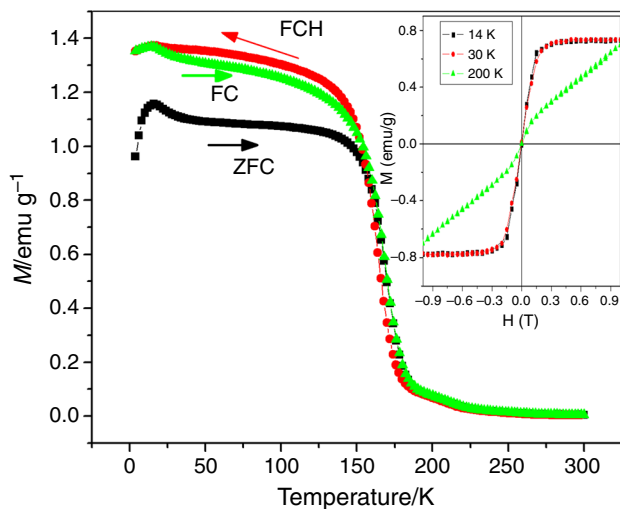


Fig. 2 Magnetization (M) versus temperature measurement in the temperature range 2–300 K under ZFC–FC–FCW protocols showing the re-entrant transition at charge-ordered state. Inset shows the M – H measurement results on $\text{Nd}_{0.3}\text{Sm}_{0.2}\text{Sr}_{0.5}\text{MnO}_3$ carried out at 14, 30, and 200 K showing ferromagnetic behavior at lower temperatures and mixed state at 200 K

the Rietveld profile refinement program. The goodness of the fits was found to be around 1.25. To estimate the $\text{Mn}^{3+}/\text{Mn}^{4+}$ ratio, iodometric redox titrations were carried out. It was found from the titration that there was a small excess content of oxygen. Lattice parameters and titration results are shown in Table 1.

Magnetization measurement

Figure 2 shows how the DC magnetization varied with temperature in the temperature range of 2–300 K for the sample of $\text{Nd}_{0.3}\text{Sm}_{0.2}\text{Sr}_{0.5}\text{MnO}_{3+\delta}$ under zero field cooled (ZFC), field cooled (FC), and field cooled heating (FCH) protocols at an applied field of 0.1 T as measured with a Quantum Design Superconductor Quantum Interference Design (SQUID) magnetometer. Results showed a large bifurcation between the ZFC and FC measurements indicating a local anisotropy in the samples. Transition temperatures (T_C or T_N) were calculated (given in Table 2) from the differential change of the DC magnetization with the temperature (dM/dT). FC–ZFC curves separated from each other at a temperature that could be explained as the irreversibility temperature, T_{irr} ($T_{\text{irr}} < T_C$). The low field ZFC curve clearly showed a cusp at so called freezing (or spin glass) temperature, T_g [11]. We suppose that CO and AFM spin ordering at Mn sites exist in the sample. Transition from ferromagnetic metal to AFM insulator suggested that there was considerable mismatch effect located at A-site cations [12]. Accordingly, for $\text{Ln}_{0.5}\text{A}_{0.5}\text{MnO}_3$

Table 2 T_C , T_{CO} , and T_{irr} of the NSSMO estimated from M – T data of Fig. 2

Sample	T_C/K	T_{CO}/K	T_{irr}/K
$\text{Nd}_{0.3}\text{Sm}_{0.2}\text{Sr}_{0.5}\text{MnO}_3$	167	200	150

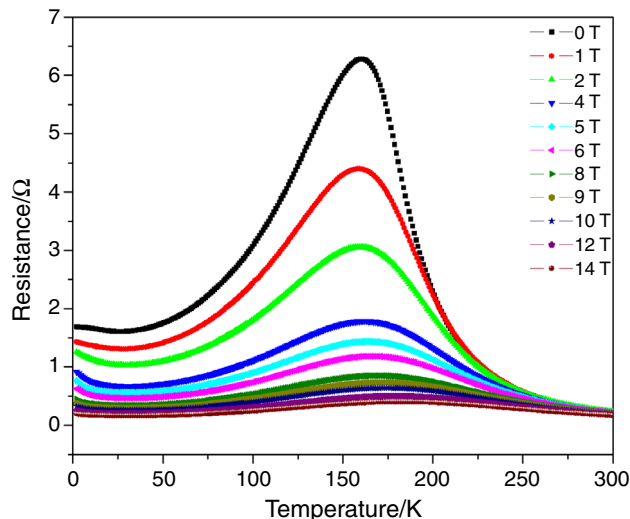


Fig. 3 Electrical resistance versus temperature of series $\text{Nd}_{0.3}\text{Sm}_{0.2}\text{Sr}_{0.5}\text{MnO}_3$ showing peaks due to semiconductor to metal transitions at ~ 150 K under all applied magnetic fields up to 14 T

perovskite, the drastic changes in properties were seen over the small range of $\langle r_A \rangle$, from 0.109 to 0.112 nm.

The isothermal magnetic hysteresis loop (M – H) of the sample (inset of Fig. 2) observed with an applied magnetic field of 1 T and at different temperatures (14, 30, and 200 K) revealed a temperature-dependent phase change. Ferromagnetic phase did not completely extend to the whole volume of the sample and it resulted in increased value of M for the same magnetic field as found by Meihua, Xu et al. [13]. That was due to canting of magnetic spins amongst Mn^{3+} – Mn^{4+} ions; which is common in manganites with 50 % Sr doping [1]. Similar reports were given recently by Chatterjee et al. [14].

Electrical resistance measurement

Electrical resistance versus temperature (T) measurements were performed at an applied magnetic field of 0–14 T and in the temperature range of 2–300 K and are shown in Fig. 3. Resistance versus T curves showed a peak at ~ 150 K for all applied fields. Maximum value of resistance was found in the absence of applied external magnetic field and it decreased as the applied magnetic field increased from 0 to 14 T. This kind of peak in the

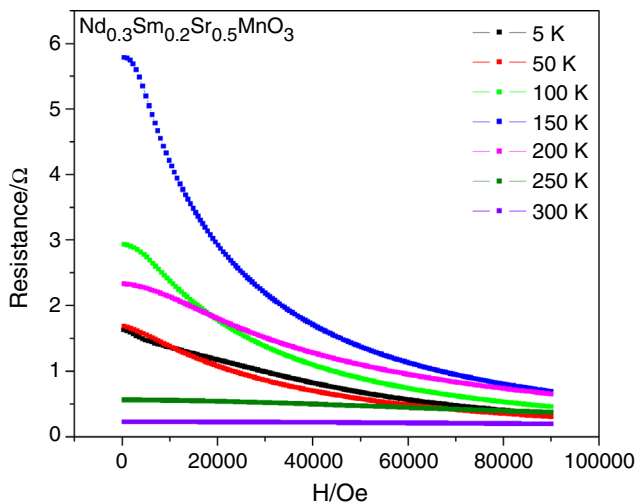


Fig. 4 Electrical resistance of the sample $\text{Nd}_{0.3}\text{Sm}_{0.2}\text{Sr}_{0.5}\text{MnO}_3$ versus magnetic field showing a maximum magnetoresistance at 150 K due to semiconductor to metal transitions

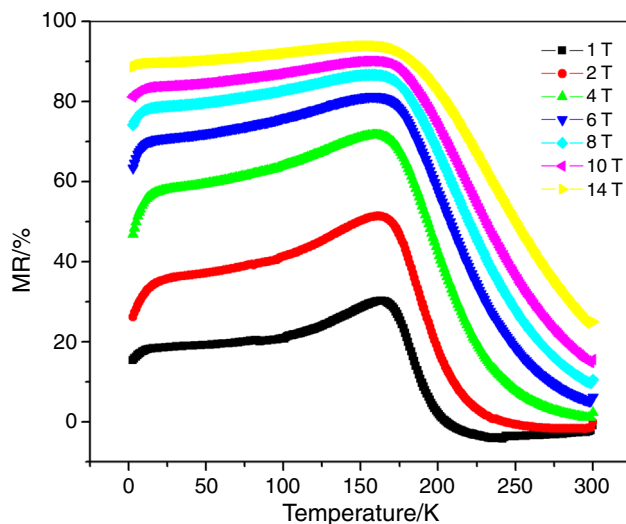


Fig. 5 Plot of magnetoresistance (MR) versus temperature showing peaks at ~ 150 K

resistivity with temperature occurs in the region where the material goes through a metal to insulator phases change through charge ordering of Mn^{3+} and Mn^{4+} ions. In some ferromagnetic materials with suitable doping, this kind of features was observed by Kimura et al. [15]. It can be concluded that at ~ 150 K there was a transition, which may be attributed to charge ordering of Mn^{3+} and Mn^{4+} ions and leading to a metal-insulator transition. Field dependent broadening of peak indicated the ferromagnetic-like ordering of rare earth ions. This is observed in many ferromagnetic materials near the ferromagnetic transition

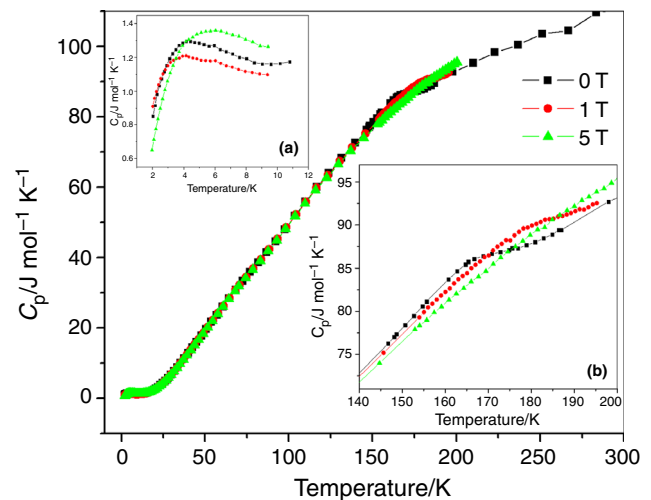


Fig. 6 C_p versus temperature of the $\text{Nd}_{0.3}\text{Sm}_{0.2}\text{Sr}_{0.5}\text{MnO}_3$ showing peaks at 160–180 K due to semiconductor to metal transitions in *inset* (b) and a shoulder in low-temperature specific heat below 7 K in *inset* (a)

[16]. This can further be verified by the thermodynamic measurements.

Figure 4 shows the resistance versus magnetic field ($R-H$) plot at 5, 50, 100, 150, 200, 250, and 300 K with varying applied magnetic field of 0–10 T. At 150 K, the trend showed the highest resistance at low fields and very low resistance at high field, which was in clear agreement with earlier statement of metal-insulator transition. It can also be concluded that the transition below 200 K exhibited the metal-insulator transition and at 150 K, there were different trends clearly indicating the kinetic arrest state of the spins. Temperature beyond 250 K showed the absence of this feature due to spin melting of AFM cluster in this range of temperatures. Up to 200 K, these measurements showed a similar observation but the magnitude of the resistance was highest at 150 K and it decreased toward low temperature and low fields. It can also be seen that the effect of magnetic field played a vital role to flip the spins rapidly and gave clear signs of the magnetoresistance changes with the temperature in the present system as given in Fig. 5.

Specific heat measurement

Figure 6 shows the variation of specific heat data of NSSMO with the temperature at different magnetic fields of 0, 1, and 5 T. From the figure, it is clearly observed that there were two transitions in the sample, which are clearly shown in the insets of Fig. 6. It was found that the low-temperature specific heat (LTSH) values were high. These values were similar to those reported by Gordon et al. [17].

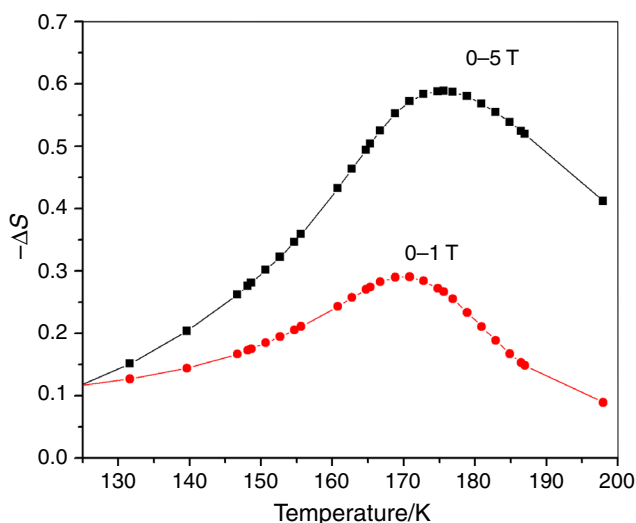


Fig. 7 Magnetic entropy change ΔS_M of NSSMO as a function of temperature for a field variation from 0–1 to 0–5 T

Under zero magnetic field, the LTSH showed a significant shoulder below 7 K (inset of Fig. 6a). The hump was still distinguishable even under magnetic field of 5 T. This feature is attributed to the Schottky-like anomaly due to the transmitting of electrons in the splitting energy levels of Nd³⁺ ion [18, 19] and is related with the Kramers theorem, which states that an ion possessing an odd number of electrons, no matter how unsymmetrical the crystal field may be, must have a ground state that is at least doubly degenerate. The anomaly at 165 K (inset of Fig. 6b) was due to the charge ordering, and the high temperature transition was affected by the magnetic fields. It indicates that the entropy of the system was shifting to higher temperatures.

Calculation of MCE

When a magnetic material is magnetized by the application of a magnetic field, the magnetic energy associated with the magnetic degrees of freedom is changed and the so called magnetic entropy change, $\Delta S_M(T) = S(T)_H - S(T)_0$, can be estimated from calorimetric measurements by integration:

$$\begin{aligned} \Delta S_M(T, H) &= S(T)_H - S(T)_0 \\ &= \int \{C_p(T)_H/T - C_p(T)_0/T\}dT, \end{aligned} \quad (1)$$

where $S(T)_H$ and $S(T)_0$ are the entropy values, whereas $C_p(T)_H$ and $C_p(T)_0$ are the heat capacity values measured in field H and in zero field, respectively. Usually, applying a magnetic field to a FM material will lower its magnetic entropy. The entropy change, $-\Delta S_M(T, H)$, as a function of temperature in the range of 125–200 K for different

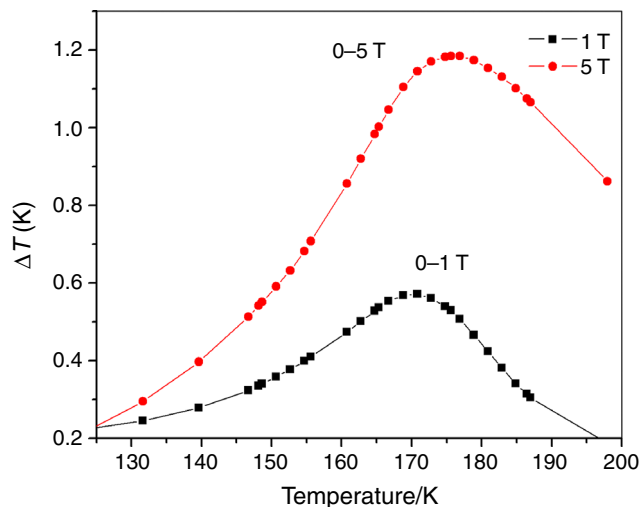


Fig. 8 The calculated adiabatic temperature change in NSSMO

Table 3 Calculated values of the maximum magnetic entropy change $(\Delta S)_{\max}$ and the maximum adiabatic temperature change $(\Delta T)_{\max}$ from Figs. 7 and 8

S. no.	$(\Delta S)_{\max}/K$	$(\Delta T)_{\max}/K$
1 T	170	170
5 T	176	175

magnetic fields is shown in Fig. 7. The $-\Delta S_M$ ran over the positive $-\Delta S_M$ values expected for the conventional magnetocaloric effect, going through the maximum value of 0.3 and 0.58 J mol⁻¹ K at a temperature of 170 K for the fields of 1 and 5 T, respectively. A slight increase in the temperature of the maximum of $-\Delta S_M$ at higher magnetic field of 5 T seen in Fig. 7 would correspond to the slight increase in the transition temperature seen through magneto-resistance measurement (Fig. 5). Results for MCE in terms of an adiabatic temperature change (ΔT_{ad}) for different magnetic field change are displayed in Fig. 8. Table 3 shows that the maximums of magnetic entropy change $(\Delta S)_{\max}$ and adiabatic temperature change $(\Delta T)_{\max}$ increased slightly from 170 to 175 K as the magnetic field was increased from 1 to 5 T. These temperatures also corresponded the transition temperature, T_C , of ~ 160 –185 K (Table 2) measured at 0.1 T. The peak of the curve corresponds to $\Delta T_{\text{ad}} = 0.5$ and 1.2 K for a field change of 1 and 5 T, respectively, and the results are in comparable with the literature [9].

Conclusions

Sm-doping at the rare earth A-site of the half doped charge-ordered manganite Nd_{0.3}Sm_{0.2}Sr_{0.5}MnO₃ has been studied.

On such doping, there was not much structural distortion found as compared with the standard $\text{Nd}_{0.5}\text{Sr}_{0.5}\text{MnO}_3$ sample. Semiconductor to insulator transition was correlated to magnetic and electrical properties, which was a clear indication of PM to FMM and FMM to AFI transition. Magnetocaloric nature of NSSMO satisfies some important criteria for selecting magnetic refrigerants such as exhibition of large magnetic entropy change and large adiabatic temperature change.

Acknowledgements The authors are grateful to DRDO, Govt. of India for supporting the present research work through a Research project (No. EPR/ER/0803750/M/01/1207). Second author thanks CSIR for providing fellowship. We also thank the Director, UGC-DAE CSR, Indore and Dr. D. Das, Dr S Chatterjee, and Mr P V Rajesh, UGC-DAE CSR, Kolkata, Prof R K Kotnala, Dr Jyoti Shah, NPL, Delhi and Prof D Varshney, DAVV, Indore for their valuable discussions, encouragement, and guidance. We acknowledge the funding of DST, Government of India, for providing funds to the PPMS and MPMS facility at CSR India.

References

- Rao CNR, Raveau B. Colossal magneto resistance charge ordering and related properties of manganese oxides. 1st ed. Singapore: World Scientific; 1998.
- Tokura Y. Colossal magnetoresistive oxides. 1st ed. New York: Gordon and Breach Science; 2000.
- Zener C. Interaction between the d-shells in the transition metals. *Phys Rev B*. 1951;82:403.
- Mavani KR, Paulose PL. Effects of cation disorder and size on metamagnetism in A-site substituted $\text{Pr}_{0.5}\text{Ca}_{0.5}\text{MnO}_3$ system. *Appl Phys Lett*. 2005;86:162504.
- Wang KF. A-site disorder induced collapse of charge-ordered state and phase separated phase in manganites. *App Phys Lett*. 2006;89:222505.
- Dagotto E. Nanoscale phase separation and colossal magnetoresistance. 1st ed. New York: Springer; 2002.
- Coey M. Charge-ordering in oxides. *Nat Mater*. 2004;430:156–7.
- Martinez LMR, Attfield JP. Cation disorder and size effect in manganese oxide perovskites. *Phys Rev B*. 1996;54:R15622–5.
- Phan MH, Yu SC. Review of the magnetocaloric effect in manganite materials. *J Magn Magn Mater*. 2007;308(2):325–40.
- Hamad M. Magnetocaloric properties of $\text{La}_{0.6}\text{Ca}_{0.4}\text{MnO}_3$. *J Therm Anal Calorim*. 2013;113(2):609–13.
- Chau N, Tho ND, Luong NH, Giang BH, Cong BT. Spin glass-like state, charge ordering phase diagram and positive entropy change in $\text{Nd}_{0.5-x}\text{Pr}_x\text{Sr}_{0.5}\text{MnO}_3$. *J Magn Magn Mater*. 2006;303:e402–5.
- Mathieu R, Akahoshi D, Asamitsu A, Tomioka Y, Tokura Y. Colossal magnetoresistance without phase separation: disorder-induced spin glass state and nanometer scale orbital-charge correlation in half doped manganites. *Phys Rev Lett*. 2004;93:227202–4.
- Xu M, Hu X, Yu J, Cui X, Zhang S. Magnetoresistance and magnetostriction effect of $(\text{La}_{1-x}\text{Sm}_x)_{2/3}\text{Sr}_{1/3}\text{MnO}_3$ manganites. *Solid State Commun*. 2008;148:217–20.
- Chatterjee S, Giri S, Majumdar S. Metastability and inverse magnetocaloric effect in doped manganite $\text{Nd}_{0.25}\text{Sm}_{0.25}\text{Sr}_{0.5}\text{MnO}_3$ and ferromagnetic shape memory alloy $\text{Ni}_2\text{Mn}_{1.36}\text{Sn}_{0.64}$: a comparison. *J Phys Condens Matter*. 2012;24(36):366001.
- Kimura T, Shintani H, Arima T, Takahashi KT, Ishizaka K, Tokura Y. Distorted perovskite with e_g^1 configuration as a frustrated spin system. *Phys Rev B*. 2003;68(060403):1–4.
- Kumar NP, Reddy PV. Specific heat and magnetization studies of RMnO_3 (R = Sm, Eu, Gd, Tb and Dy) multiferroics. *Phys Scr*. 2011;83(045701):1–8.
- Gordon JE. Specific heat of $\text{Nd}_{0.67}\text{Sr}_{0.33}\text{MnO}_3$. *Phys Rev B*. 1999;59(1):127–30.
- Swamy NK, Kumar NP, Gupta M, Malik V, Das BK. Schottky-like anomaly in the low-temperature specific heat of polycrystalline $\text{Y}_{0.3}\text{Gd}_{0.2}\text{Sr}_{0.5}\text{MnO}_3$. *Mater Phys Mech*. 2013;18:35–41.
- Cheng JG, Sui Y, Qian ZN, Liu ZG, Miao JP, Huang XQ, Lu Z, Li Y, Wang XJ, Su WH. Schottky-like anomaly in the low-temperature specific heat of single-crystal NdMnO_3 . *Solid State Commun*. 2005;134(6):381–4.